(7) Wegner, G. *Pure Appl. Chem.* **1977**, *49*, 443.
(8) Baughman, R. H.; Yee, K. C. *J. Polym. Sci., Macromol. Rev.* **1978**, *13*, 219.
(9) Enkelman, V. In "Recent Advances in the Quantum Theory of Polymers"; André, J.-M., Brédas, J.-L., Delhalle, J., Ladik, J., Leroy, G., Moser, C., Eds.; Springer-Verlag: Berlin, 1980; p 1.
(10) Baughman, R. H. In "Contemporary Topics in Polymer Science"; Pearce, E. M., Schaefgen, J. R., Eds.; Plenum Press: New York, 1977; Vol. 2, p 205.
(11) Schermann, W.; Wegner, G. *Makromol. Chem.* **1974**, *175*, 667. Wegner, G.; Schermann, W. *Colloid Polym. Sci.* **1974**, *252*, 655.
(12) Chance, R. R.; Baughman, R. H. *J. Chem. Phys.* **1976**, *64*, 3889.
(13) Siddiqui, A. S.; Wilson, E. G. *J. Phys. C* **1979**, *12*, 4237.
(14) Bloor, D.; Hubble, C. L.; Ando, D. J. In "Molecular Metals", NATO Conference Series IV; Hatfield, W., Ed.; Plenum Press: New York, 1979; p 243.
(15) Seiferheld, U.; Bassler, H. *Solid State Commun.* **1983**, *47*, 391.
(16) Patel, G. N. *Polym. Prep. (Am. Chem. Soc., Div. Polym. Chem.)* **1978**, *19*, 154; Patel, G. N.; Walsh, E. K. *J. Polym. Sci., Lett. Ed.* **1979**, *17*, 203. Patel, G. N. *J. Chem. Phys.* **1979**, *70*, 4387.
(17) Se, K.; Ohnuma, H.; Kotaka, T. *Polym. J.* **1982**, *14*, 895.
(18) Se, K.; Ohnuma, H.; Kotaka, T. *Macromolecules* **1983**, *16*, 1581.
(19) Ohnuma, H.; Inoue, K.; Se, K.; Kotaka, T. *Macromolecules* **1984**, *17*, 1285.
(20) Hay, A. S. *J. Org. Chem.* **1962**, *27*, 3320.
(21) Adachi, K.; Hirose, Y.; Ishida, Y. *J. Polym. Sci.* **1975**, *13*, 737.
(22) Patel, G. N.; Miller, G. G. *J. Macromol. Sci.-Phys.* **1981**, *B20*, 111.
(23) Saito, S.; Sasabe, H.; Nakajima, T.; Yada, K. *J. Polym. Sci., Part A-2* **1968**, *6*, 1297.
(24) Blythe, A. R. "Electrical Properties of Polymers"; Cambridge University Press: Cambridge, U.K., 1979.
(25) Bhatt, A. P.; Anderson, W. A.; Kang, E. T.; Ehrlich, P. *J. Appl. Phys.* **1983**, *54*, 3973.
(26) Wenz, G.; Wegner, G. *Makromol. Chem., Rapid Commun.* **1982**, *3*, 231.
(27) Patel, G. N.; Lee, L. T. C. *J. Macromol. Sci.-Phys.* **1983**, *B22*, 259.

Local Conformation of Poly(methyl methacrylate) by Intermediate-Angle X-ray Scattering

Saburo Yamaguchi, Hisao Hayashi, Fumiyuki Hamada,* and Akio Nakajima

Department of Polymer Chemistry, Kyoto University, Kyoto 606, Japan.
Received December 15, 1983

ABSTRACT: Local conformations of poly(methyl methacrylate) (PMMA) chains in solution have been investigated by intermediate-angle X-ray scattering. Scattered intensity was measured for atactic and syndiotactic PMMA dissolved in benzene, acetone, and 3-heptanone (Θ-solvent) and placed on an absolute scale with reference to the primary beam intensity. The theoretical scattering functions were also calculated by use of the rotational isomeric state scheme based on the conformation energies calculated by Sundararajan and Flory. All atoms effective to X-ray scattering were incorporated in the calculations. The effect of the electron density of the solvent was also taken into account but found to have no major influence on the scattering curves. Although the theoretical scattering functions based on the ordinary two-state scheme can reproduce major features of the experimental scattering functions, quantitative agreement was inadequate. Adoption of an increased number of rotational isomeric states (14-state scheme) was found to fail in reducing this discrepancy. In an attempt at readjusting the molecular parameters in favor of the accordance between the theory and experiments, considerably better agreement was observed when a larger skeletal bond angle ($\theta' = 53°$) at the dyad was assumed. This readjusted angle, however, seems to be slightly beyond the uncertainty of the conformation energy calculations. Therefore we are led to suspect the existence of specific long-range interactions, which annihilate the simple statistical mechanical treatment, owing to specific characteristics of the chain.

Introduction

The methods[1] of determining overall conformations of polymer chains in solution have fully been established; e.g., the radius of gyration of the polymer chain can be determined by light scattering[2] with accuracy. A vast body of information thereby accumulated provides foundations for comprehensive theories of polymer solutions. On the other hand, little is known about local conformations, or conformations in short bond sequences within polymer chains, despite their importance for elucidating conformation-dependent properties on a molecular level. Scattering of X-rays and neutrons,[3] mean-square dipole moments, and optical anisotropy are known to depend on such local conformations.[4] In particular, intermediate-angle X-ray scattering (IAXS)[4] corresponding to a Bragg spacing of about 5–50 Å has been proven to be sensitive to correlations between the loci of atoms separated by short bond sequences and hence to the local conformations.

The conformation of poly(methyl methacrylate) (PMMA) in solution has been studied by many investigators. Kirste and co-workers[5–7] measured X-ray and neutron scattering from PMMA of different tacticities in solution and in bulk and observed oscillation in the scattering curve at intermediate angles for the syndiotactic chain. They attributed this peculiarity to a helical feature of the local chain conformation based on the calculations of the scattering functions of wormlike chains with persistence of curvature.[8] Yoon and Flory[9,10] also calculated the scattering function of syndiotactic PMMA using a more realistic model based on conformational energy calculations[11] and the rotational isomeric state (RIS) scheme.[12] Whereas their calculation[10] of the neutron scattering function was performed by treating methyl and methylene groups as scattering elements, the X-ray scattering function was calculated with α carbons regarded as the scattering loci. Since the choice of the scattering elements is of crucial importance in the precise calculations of the scattering functions at intermediate angles,[13] it is desirable to calculate the X-ray scattering functions by taking into account all effective atoms explicitly.

In this paper we performed absolute measurements of IAXS by syndiotactic and atactic PMMA in benzene,

0024-9297/84/2217-2131$01.50/0

Table I
Molecular Characterization of the Samples

a-PMMA		s-PMMA	
$M_w = 1.45 \times 10^5$ $M_w/M_n = 1.38$		$M_v = 4.8 \times 10^4$	
$i = 4\%$ $h = 32\%$ $s = 64\%$	$w_m = 0.20$ $w_r = 0.80$	$i = 1\%$ $h = 22\%$ $s = 77\%$	$w_m = 0.12$ $w_r = 0.88$

acetone, and 3-heptanone and compared them with the scattering functions calculated by the RIS scheme treating all carbon and oxygen atoms as point scatterers. Furthermore, as we have pointed out,[14] ordered local conformations could be exaggerated when the assigned number of the RIS is very small. In this connection we calculated the persistence vector,[15] second moment, and scattering function employing an increased number of the RIS in order to avoid overestimation of an ordered conformation, i.e., the all-trans planar conformation, which is statistically preferred in the ordinary two-state scheme employed by Flory and co-workers.[9-11] The local conformations of PMMA chains are discussed from the conformational point of view in connection with results obtained by other experiments.

Experimental Section

Materials. Atactic PMMA (a-PMMA) was prepared by the solution polymerization of methyl methacrylate in carbon tetrachloride using 2,2′-azobis(isobutyronitrile) as an initiator, fractionated into five fractions in acetone at 30 °C using methanol as precipitant, and dried under vacuum at 40 °C. The middle fraction was used for the scattering measurements. Syndiotactic PMMA (s-PMMA) was purchased from Polyscience Ltd. (lot no. 23491), fractionated into four fractions, and dried similarly. The upper middle fraction was used for the scattering measurements. The molecular weight distribution and average molecular weight of a-PMMA were measured by GPC with a Shimazu GPC-100 in tetrahydrofuran solution. The molecular weight of s-PMMA was measured by viscometry.[16] The fraction w_m of the meso dyad was determined by ^{1}H NMR with a JEOL FX90Q in chlorobenzene at 120 °C.[17] The results of characterization of the samples are summarized in Table I.

Analytical grade benzene and acetone were used without further purification. Reagent grade 3-heptanone, which is a Θ-solvent for PMMA at 30–34 °C,[18,19] was dried over potassium carbonate and fractionally distilled.

X-ray Scattering Measurements. Measurements of X-ray scattering were made with a Kratky U-slit camera using a Cu-anode tube as an X-ray source. Scattered intensity was measured with a scintillation counter equipped with a pulse height analyzer and with a 10 μm Ni β filter. The counter was scanned stepwise by means of a full-automatic step controller. About 40 steps were scanned for each curve, and 5×10^5 to 2×10^6 pulses were collected at each scattering angle. Since the primary beam with a line-shaped cross section was used to obtain high scattered intensity, the collimation error must be corrected (desmeared). The iterative method of Glatter[20] was used for this purpose. A thin-walled quart capillary of about 0.2-cm diameter was used as a container of the solution. In order to place the Kratky function on an absolute scale, the total intensity P of the primary beam was measured with a secondary standard sample, Lupolen platelet, calibrated by Kratky and co-workers.[21] The excess scattering cross section $d\Sigma/d\Omega$ per unit volume of the sample is determined by the excess scattered intensity I through the reaction

$$d\Sigma/d\Omega = (I/P)(r^2/dT) \tag{1}$$

where r is the sample-to-detector distance, d is the thickness of the sample, and T is the transmission. The absolute Kratky function $F_x(h)$,[13,22] which will be defined in the next section, can be experimentally evaluated by the equation

$$F_x(h) = \frac{(d\Sigma/d\Omega)h^2}{KcM_u} \tag{2}$$

where c is the concentration of the solution in g/cm^3, M_u is the molecular weight of the monomer unit, and K is a constant given by

$$K = i_e(z_2 - \bar{v}_2\rho)^2 N_A \tag{3}$$

where i_e is the Thomson constant, or the scattering cross section of a free electron, 7.94×10^{-26} cm^2, z_2 is the mole electron in 1 g of the polymer, $\bar{v}_2$ is the partial specific volume of the polymer, ρ is the electron density of the solvent, and N_A is Avogadro's number. The measurement of s-PMMA in 3-heptanone was not performed because s-PMMA did not dissolve below 40°C. The concentrations of the samples are 0.0205 g/cm^3 for a-PMMA in acetone, 0.0192 g/cm^3 for a-PMMA in 3-heptanone, 0.0194 g/cm^3 for a-PMMA in benzene, 0.0194 g/cm^3 for s-PMMA in acetone, and 0.0185 g/cm^3 for s-PMMA in benzene. A measurement of a-PMMA in 3-heptanone was made at 31 ± 0.01 °C and other measurements were made at 25 ± 0.01 °C.

Partial Specific Volume. The partial specific volume $\bar{v}_2$ of a-PMMA in 3-heptanone was measured at 30 °C with a Shibayama Kagaku digital densitometer and determined to be 0.835 cm^3/g. The values of $\bar{v}_2$ in acetone and in benzene are 0.812 and 0.807 cm^3/g, respectively, according to the literature.[23]

Theoretical Scattering Functions

The scattering function for a system of randomly oriented independent molecules comprising $x + 1$ identical units is given by

$$P(h) = (x+1)^{-2}\left(\sum_k^{n_u} f_k\right)^{-2} \sum_{i,j}^{x+1} \sum_{k,l}^{n_u} f_k f_l \left\langle \frac{\sin(hr_{ij;kl})}{hr_{ij;kl}} \right\rangle \tag{4}$$

where $r_{ij;kl}$ is the distance between the kth atom in the ith unit and the lth atom in the jth unit, f_k is the excess scattering factor of the kth atom, n_u is the number of effective atoms in the unit, h is the magnitude of the scattering vector defined by $h = (4\pi/\lambda)\sin\theta$, θ being half of the scattering angle, and the angular brackets denote the statistical average over all conformations of the chain. If we assume that $\langle \sin(hr_{ij;kl})/hr_{ij;kl} \rangle$ is independent of the location of the sequence of $t = |i - j|$ units, the scattering function can be rewritten as

$$P(h) = (x+1)^{-2}\left(\sum_k^{n_u} f_k\right)^{-2} \sum_t^{x} \sum_{k,l}^{n_u} 2(x+1-t) f_k f_l \left\langle \frac{\sin(hr_{t;kl})}{hr_{t;kl}} \right\rangle \tag{5}$$

Avoiding difficulties in evaluating all terms in eq 5, we may introduce an approximation

$$\left(\sum_k^{n_u} f_k\right)^{-2} \sum_{k,l}^{n_u} f_k f_l \left\langle \frac{\sin(hr_{t;kl})}{hr_{t;kl}} \right\rangle = \left\langle \frac{\sin(hr_t)}{hr_t} \right\rangle \tag{6}$$

where r_t is the distance between representative atoms (e.g., C^α) in the ith and jth units separated by t units ($|i - j| = t$). The approximation is valid for large values of t exceeding a certain limit t_0, which can be estimated by comparison of the left-hand and right-hand terms in eq 6. Substitution of eq 6 into eq 5 leads to

$$P(h) = (x+1)^{-2}\left(\sum_k^{n_u} f_k\right)^{-2} \left[\sum_{t=0}^{t_0} 2(x+1-t) \times \sum_{k,l}^{n_u} f_k f_l \left\langle \frac{\sin(hr_{t;kl})}{hr_{t;kl}} \right\rangle + \left(\sum_k^{n_u} f_k\right)^2 \sum_{t=t_0+1}^{x} 2(x+1-t) \left\langle \frac{\sin(hr_t)}{hr_t} \right\rangle \right] \tag{7}$$

Table II
Values of $\bar{V}$, V_k, f_k^0, and f_k for PMMA in Benzene

atom	$\bar{V}_k$,[a] cm³/mol	V_k,[b] cm³/mol	f_k^0	f_k
—C(—)—	3.33	4.74	6	3.77
>CH₂	10.23	14.56	8	1.15
—CH₃	13.67	19.46	9	−0.16
>C=	5.01	7.13	6	2.65
O=	6.70	9.54	8	3.51
—O—	5.50	7.83	8	4.32

[a] Reference 27. [b] V_k is obtained according to the equation[14] $V_k = M_u\bar{v}_2\bar{V}_k/(\Sigma\bar{V}_k)$.

The second terms in the brackets in eq 7 can be expanded in a series form[24-26]

$$\left\langle \frac{\sin(hr_t)}{hr_t} \right\rangle = \exp\left(-\frac{\langle r_t^2\rangle h^2}{6} \right) \sum_{m=0}^{\infty} g_{2m} \left(\frac{\langle r_t^2\rangle h^2}{3} \right)^m \quad (8)$$

where g_{2m} is an expansion coefficient defined by

$$g_{2m} = \begin{cases} 1 & (m = 0) \\ 2^{-m} \sum_{j=1}^{m} \frac{(-1)^{j-1}}{j!(m-j)!} \left(1 - \frac{3^j\langle r_t^{2j}\rangle}{(2j+1)!!\langle r_t^2\rangle^j} \right) & (m \geq 1) \end{cases} \quad (9)$$

and $\langle r_t^{2p}\rangle$ is the $2p$th moment of the ith and jth units separated by t units ($|i-j| = t$). The scattering function for PMMA chains was calculated by eq 7 in combination with eq 8 and 9.

The absolute Kratky function defined by[13,22]

$$F_x(h) = (x+1)h^2P(h) \quad (10)$$

is useful to discusss the shape and magnitude of the scattering function at intermediate angles on an absolute scale.

Numerical Calculations

Two-State Scheme. Geometrical parameters and the torsion angles for two rotational isomeric states, $\varphi_t = 0°$ and $\varphi_g = 120°$, were assigned according to Sundararajan and Flory.[11] The statistical weights were evaluated by using the optimized energies $E_\alpha = 1100$ and $E_\beta = -600$ cal/mol.[11] The conformation for planar ester group was fixed so that the CH_3–C bond may be cis to the C=O bond. All carbon and oxygen atoms were regarded as point scatterers, which facilitates evaluation of the effective scattering power of each atom in solution. We estimated the excess scattering factor f_k by a primitive method reported in a previous paper[14] according to the equation

$$f_k = f_k^0 - \rho V_k \quad (11)$$

where f_k^0 is the atomic scattering factor equivalent to the atomic number of the kth atom, ρ is the mole electron density of solvent, and V_k is the molar volume of the kth atom. Values of V_k are calculable from the van der Waals volume $\bar{V}_k$[27] and partial specific volume. Results of the estimation of f_k for PMMA in benzene are summarized in Table II.

In order to apply eq 7 we estimated the value of t_0 by Monte Carlo calculations. The right-hand and left-hand terms in eq 6 were compared by changing the value of t, and the minimum value of t that fulfills eq 6 was taken as t_0. We obtained $t_0 = 41$ for a-PMMA but used a sufficiently large value $t_0 = 50$ in calculations hereafter for both a-PMMA and s-PMMA. The scattering functions of s-PMMA were calculated for chains of $x = 1000$. The term $\langle \sin(hr_t)/hr_t \rangle$ ($t \leq 50$) was evaluated as an average over 5000 Monte Carlo chains comprising t units ($t = 1$–50) embedded in longer chains of $100 + t + 100$ units, each chain being generated according to the conditional probabilities.[10] The term $\langle \sin(hr_t)/hr_t \rangle$ ($t > 50$) was calculated by eq 8 truncated at the term including $\langle r_t^8 \rangle$, with the even moments $\langle r_t^{2p} \rangle$ evaluated by the generator matrix method.[28] Truncation error of the moment expansion was determined to be small by comparing with the Monte Carlo data at $t = 50$.

The scattering function of a-PMMA chains of meso dyad fraction $w_m = 0.2$ was also calculated for $x = 1000$, assuming a Bernoullian distribution of meso and racemic dyads. The term $\langle \sin(hr_t)/hr_t \rangle$ ($t \leq 50$) was calculated as an average over conformations and over stereochemical configurations; for each of 40 stereochemical configurations generated by the Monte Carlo method, 500 Monte Carlo conformations were generated (total of 20 000 conformations for each value of t) according to the conditional probabilities for each configuration. To avoid the application of the equivalent freely jointed chain model[29] to the evaluation of $\langle \sin(hr_t)/hr_t \rangle$, we calculated the even moments up to and including $\langle r_t^8 \rangle$ for Monte Carlo chains of t units embedded in chains of $100 + t + 100$ units, with t ranging from 50 to 100 with an interval of 10. To ensure the convergence of the second moment and moment ratios, 500 conformations for each of 180 stereochemical configurations (total of 90 000 conformations for each value of t) were sufficient. The characteristic ratio $C_t = \langle r_t^2 \rangle / 2tl^2$ and moment ratios $\langle r_t^{2p} \rangle / \langle r_t^2 \rangle^p$ for other values of t (>50) were evaluated by interpolation and extrapolation of the corresponding values calculated for discrete t including those at a Gaussian limit ($t = \infty$) by the least-squares method with a linear and quadratic function of $1/t$, respectively.

14-State Scheme. The highly preferential trans conformation in s-PMMA chains imparts to the chain an ordered local conformation with high probability. The assignment of a single torsion angle to the trans state in such sequences may lead to overestimation of ordered conformations. Therefore we performed calculations with an increased number of RIS to compare them with the results obtained by the two-state scheme.

The conformational energies were calculated as a function of successive torsion angles φ_i and φ_{i+1} within a dyad with intervals of 10° using the empirical energy functions described by Sundararajan and Flory.[11] Rotational isomeric states were chosen in low-energy regions at intervals of 10°. We assigned a total of 14 states corresponding to $\varphi = -30°$, $-20°$, $-10°$, 0°, 10°, 20°, and 30° in the neighborhood of the trans conformation and $\varphi = 90°$, 100°, 110°, 120°, 130°, 140°, and 150° in the neighborhood of the gauche conformation. Values of the elements of the statistical weight matrix $\mathbf{U}''$ for the dyad bond pair were set equal to its Boltzmann factor of the conformational energy. The elements of $\mathbf{U}'$ for the bond pair flanking the substituted carbon were assumed to be unity for the tt, tg, and gt regions and zero for the gg region,[30] because these values depend only on the second-order interactions.[31]

The scattering function for s-PMMA chains was calculated by using the 14-state scheme in the similar manner as described in the two-state scheme, except that the even moments for $t > 50$ were calculated by the Monte Carlo method, because direct evaluation of the moments requires generator matrices of excessively high orders, the order of the generator matrix $\langle r_t^8 \rangle$ being 980 × 980 even in a con-

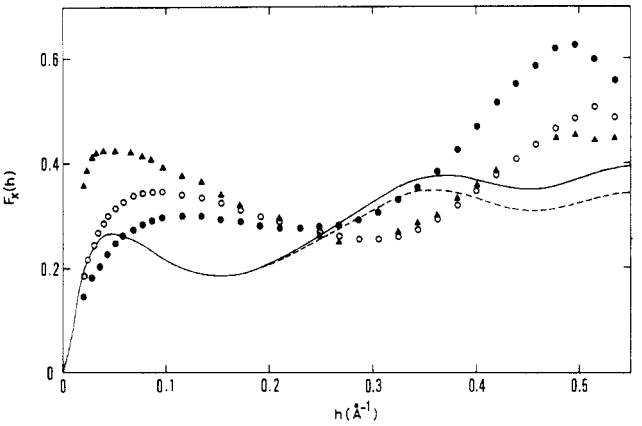

Figure 1. Kratky plots for a-PMMA in benzene (●), acetone (○), and 3-heptanone (▲). The solid curve represents the absolute Kratky function $F_x(h)$ calculated for a-PMMA chains (w_m = 0.2) by the two-state scheme with f_k estimated for PMMA in benzene. The broken curve represents the function $F_x(h)$ calculated for a-PMMA chains by the two-state scheme with f_k^0.

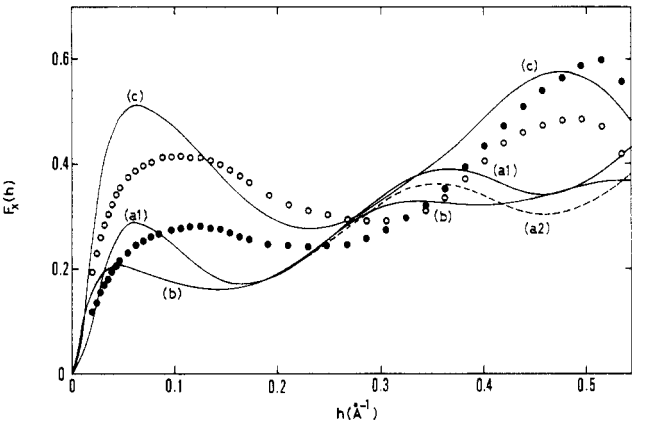

Figure 2. Kratky plots for s-PMMA in benene (●) and acetone (○). The solid curve labeled (a1) represents the absolute Kratky function $F_x(h)$ calculated for s-PMMA chains by the two-state scheme with f_k estimated for PMMA in benzene. The broken curve (a2) represents the function $F_x(h)$ calculated for s-PMMA chains by the two-state scheme with f_k^0. The solid curve labeled (b) represents the function $F_x(h)$ calculated for s-PMMA chains by the 14-state scheme with f_k. The solid curve labeled (c) represents the function $F_x(h)$ calculated for s-PMMA chains by the two-state scheme using a modified value of the angle θ' = 53° with f_k.

densed form.[32] A total of 20 000 conformations were generated for value of t according to the conditional probabilities calculated for long chains by the method of Flory and Fujiwara.[33] The characteristic ratio and moment ratios were evaluated by the extrapolation and interpolation of the values determined for t = 50–100 at intervals of 10.

To illustrate the conformational features of s-PMMA chains, the persistence vector **a**,[15] defined as the average of the end-to-end vector **r**, and the second moment $\langle r_t^2 \rangle$ were calculated by the 14-state scheme according to the generator matrix method[28] and compared with the results of the two-state shceme. Calculations of the second moment were performed for longer chains comprising 100 + t + 100 units in order to eliminate the end effect. All calculations were performed at 25 °C.

Results and Discussion

Figure 1 shows the absolute Kratky plots for a-PMMA chains. The filled and open circles and triangles represent the experimental curves measured in benzene, acetone, and 3-heptanone, respectively. The results obtained in acetone and in benzene are in good accordance with those obtained by Kirste and co-workers.[7] Since the solvent dependence in the Kratky plots at small angles ($h \lesssim 0.15$ Å^{-1}) is mainly attributed to the change in the overall chain dimensions and hence to the excluded volume effect, the comparison of the curves beyond this region is of interest. The results observed in acetone and in 3-heptanone are almost identical in the range $h \gtrsim 0.2$ Å^{-1}, where the excluded volume effect diminishes, indicating the similarity of the local conformations in these solvents. Since acetone and 3-heptanone are both polar solvents, they may interact with PMMA similarly. On the other hand, appreciable difference is observed for the benzene solution. Since the electron density of benzene (ρ = 0.470 (mol electron)/cm^3) is slightly larger than those of acetone (φ = 0.432 (mol electron)/cm^3) and 3-heptanone (φ = 0.455 (mol electron)/cm^3), a part of the difference may be attributed to this effect. However, the difference seems to be larger than expected from this effect alone (see below) and also beyond the experimental uncertainty. Therefore we infer that the local conformation of a-PMMA chains in benzene could be different from those in the other solvents. More detailed understanding of the solvent effect requires incorporation of this effect into the energy calculations as attempted by Gibson and Scherage[34] and Hopfinger.[35] Figure 1 also shows the absolute Kratky function $F_x(h)$ calculated for a-PMMA chains of w_m = 0.2. The solid curve was calculated by eq 7 with the values of f_k estimated for PMMA in benzene, and the broken curve was calculated with f_k^0 without correction for the electron density of solvent. Comparison of these two curves indicates that an increase of the electron density of solvent tends to increase the scattered intensity at intermediate angles, due to the apparent reduction of the cross section area of the chain. However, this increase in the scattering function is very small even at maximum angle shown in the figure, which assures the above inference. Although qualitative features of the experimental curves are well reproduced by the theoretical functions, quantitative agreement is unsatisfactory.

Figure 2 shows the Kratky functions for s-PMMA plotted on an absolute scale. The filled and open circles represent the experimental points obtained in benzene and in acetone, respectively, showing similar variation with solvent species as observed for a-PMMA. Figure 2 also includes theoretical Kratky function $F_x(h)$ calculated for s-PMMA chains. The solid curve (a1) was calculated by eq 7 with the values of f_k estimated for PMMA in benzene, and the broken curve (a2) was calculated with f_k^0. The agreement between the theoretical and experimental curves is only qualitative as in former calculations by Yoon and Flory.[9,10]

The characteristic peaks in the theoretical Kratky functions must be interpreted in terms of the conformational characteristics of the chain. Because of an extreme preference for the tt conformation and of inequality in the skeletal bond angles, s-PMMA chains tend to form a loop of long trans sequences of an average length of 9 units.[31] Therefore the conformation of s-PMMA is considered to be the combination of loops in the trans states shown in Figure 3 and a few kinks caused by the gauche conformation, the former being the reason for the scattering peaks. To confirm this idea, the scattering function for a randomly oriented ring of radius r_0 is calculated according to the equation

$$P(hr_0) = \int_0^{\pi/2} J_0^2(hr_0 \sin\theta) \sin\theta \, d\theta \qquad (12)$$

where $J_0(x)$ is the Bessel function of the zeroth order, and the result is shown in Figure 4 in the form of a Kratky plot.

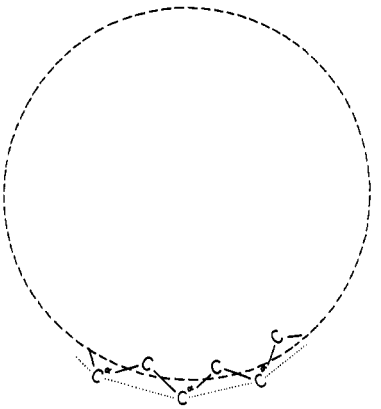

Figure 3. Schematic representation of the all-trans conformation of s-PMMA chains. The dotted lines represent virtual bonds, and the broken curve represents a ring corresponding to this conformation.

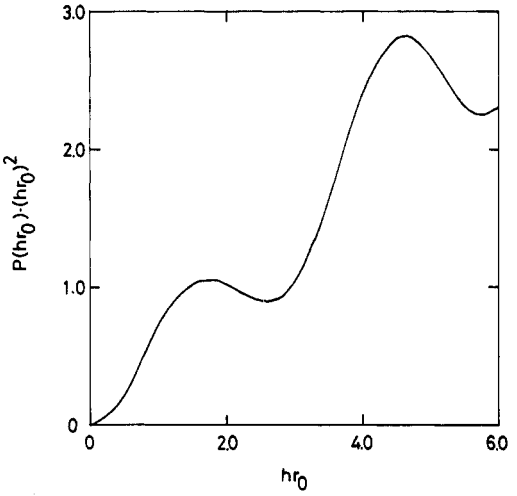

Figure 4. Scattering function calculated for a randomly oriented ring by eq 13 represented in the form of a Kratky plot, $P(hr_0)(hr_0)^2$ vs. hr_0.

The second peak appears at $hr_0 = 4.6$. If we adopt $r_0 = 12.8$ Å, which is geometrically determined for the all-trans conformation for s-PMMA, the peak occurs at about $h = 0.36$ Å^{-1}, in good accordance with the theoretical curves shown in Figure 2. Therefore we can conclude that the second peak of the theoretical Kratky functions can be understood as the consequence of the loop-forming characteristic of s-PMMA as mentioned above. Kirste[8] introduced an artificial chain with a fixed bond angle and torsion angle allowed to vary within a certain range around the cis position. The cis conformation in his model can be identified with the trans conformation in the real chain, if a virtual bond connecting the successive C^α atoms is regarded as the structural unit of the model chain (Figure 3). Therefore, Kirste's hypothetical model chains can be related to the most probable all-trans conformation in the RIS scheme.

A deeper insight into the local conformation can be gained by the persistence vector. Figure 5 shows the x–y projection of the persistence vector for s-PMMA chains. The solid curve represents the results by the 14-state scheme, and the broken curve represents those by the two-state scheme. For consistency the latter is computed with the statistical weight matrix U″ determined by the conformational energies, each element of U″ being evaluated as a sum of the Boltzmann factors calculated at intervals of 10° within the corresponding region. Since both curves are calculated from the same conformational energies, the difference must originate in the choice of the

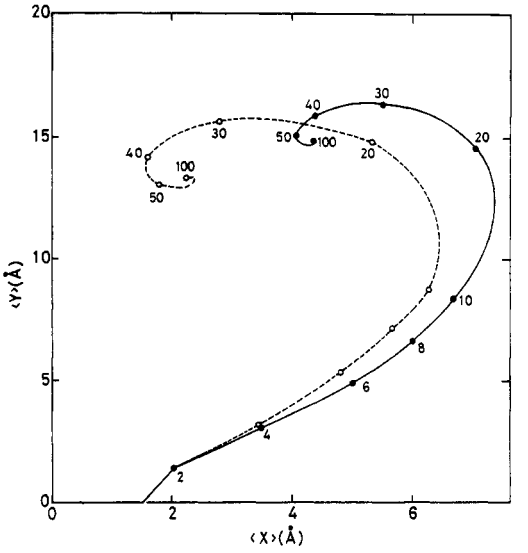

Figure 5. X and Y components of the persistence vector **a** calculated for s-PMMA chains. The solid and broken curves represent the vector calculated by the 14-state scheme and by the two-state scheme, respectively.

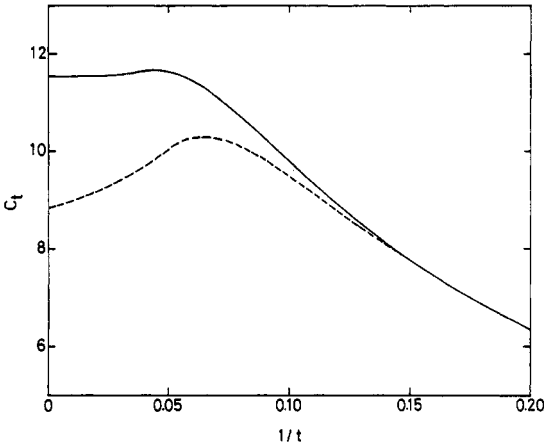

Figure 6. Characteristic ratio $C_t = \langle r_t^2\rangle/2tl^2$ calculated for s-PMMA chains. The solid and broken curves represent C_t calculated by the 14-state scheme and by the two-state scheme as a function of the reciprocal of the chain length, $1/t$.

different number of RIS. In the RIS approximation,[28,36] integrations over configuration space are replaced by the sum over a discrete set of rotational isomeric states. Therefore the more isomeric states involved, the more precise the statistical average obtained, in the sense that the fluctuation around the energy minima can be taken into account more explicitly. The appreciable difference between the two curves in Figure 5, therefore, indicates the inadequacy of employing the two-state scheme for the description of the local chain conformations. Figure 6 shows the characteristic ratio for s-PMMA chains plotted against the reciprocal of the chain length $1/t$. The solid curve is calculated by the 14-state scheme, and the broken curve by the two-state scheme. These plots suggest that the change in the number of rotational isomeric states involved appreciably affects not only local conformations but also the overall dimensions such as the second moment thereby calculated. The limiting characteristic ratio C_∞ calculated by the 14-state scheme is much larger than that obtained by the two-state scheme and hence than the experimental values.[18,19,37]

The absolute Kratky function $F_x(h)$ for s-PMMA chains calculated by the 14-state scheme is shown as the solid curve labeled (b) in Figure 2. Smaller angle dependence compared with the two-state scheme is the consequence

of the decrease of order in all-trans sequences, though loop-forming tendency is still maintained. Quantitative agreement with the experiments is not improved. As an attempt to reproduce the experimental curves, we used slightly modified values for parameters in the two-state scheme calculations. A small decrease in the conditional probability of the tt conformation does not affect the positions of scattering maxima significantly, apart from resulting flattening of the curve, as should be expected. A reasonable offset of the torsion angle for the trans state can shift the peak only slightly. Therefore no adjustment of these parameters required to fit the curves can be reconciled with the energy calculations. On the other hand, the variation of the bond angle $\pi-\theta'$ for the dyad bond pair affects the peak position appreciably, an example with $\theta' = 53°$ being shown as the solid curve labeled (c) in Figure 2. Considerable improvement in the agreement between the theory and experiments thus attained suggests that the energy calculation including bending potential terms has crucial importance. This adjustment of the bond angle is also supported by the result of wide-angle X-ray scattering measured on a-PMMA in the bulk by Lovell et al.,[38,39] who concluded that the optimum value of θ' is 52°. However, the value of the characteristic ratio $C_\infty = 4.2$ obtained for $\theta' = 53°$ is far from the experimental values, indicating that this minor change of the angle may seriously affect other conformation-dependent properties.

Another possible reason for this discrepancy is long-range interactions, which invalidate the statistical treatment of the chain conformation. PMMA chains exhibit some specific phenomena such as formation of stereocomplex between isotactic and syndiotactic chains,[40,41] and association,[42-45] as has been suggested by ^{1}H NMR spectra, osmotic pressure and viscosity measurements,[44] and light scattering[45] of s-PMMA solutions. A highly crystalline sample of s-PMMA is obtained by the solvent-induced crystallization for noncrystalline samples.[46-48] Kusuyama and co-workers[45,46] analyzed the X-ray diffraction pattern of well-oriented fibers of s-PMMA after adsorption of chloroacetone and suggested that solvent molecules are included both inside and outside the helical chains in the crystal and that these helices have a smaller radius than that of the all-trans conformation. They concluded that the basic structure of syndiotactic PMMA/solvent complexes is similar to the inclusion compounds of amylose and its derivatives such as V-amylose/Me_2SO[49] and V-amylose/water[50] complexes. These observations are all indicative of the presence of some specific long-range interactions within the s-PMMA chain. Since the racemic dyad is dominant in both samples used in this study, eventual all-trans sequences could be stabilized energetically by forming a helix of a smaller radius to occlude solvent molecules. This decrease of the radius of curvature of the chain contour can be a reason for discrepancy between the observed peak position and that calculated by the statistical theory considering only short-range interactions. Further investigations of the specific long-range interactions mentioned above and refinement of the energy calculations taking explicit account of the distortion of bond angles are required for clear understanding of the conformations of this chains in solution.

Registry No. a-PMMA (homopolymer), 9011-14-7; s-PMMA (homopolymer), 25188-97-0.

References and Notes

(1) Tanford, C. "Physical Chemistry of Macromolecules"; Wiley-Interscience: New York, 1961.
(2) Huglin, M. N., Ed. "Light Scattering from Polymer Solution"; Academic Press: New York, 1972.
(3) Higgins, J. S.; Stein, R. S. *J. Appl. Crystallogr.* **1978**, *11*, 346.
(4) Flory, P. J. *Pure Appl. Chem.* **1980**, *52*, 241.
(5) Kirste, R. G.; Kratky, O. *Z. Phys. Chem. (Wiesbaden)* **1962**, *31*, 363.
(6) Kirste, R. G. *Makromol. Chem.* **1967**, *101*, 91.
(7) Kirste, R. G.; Kruse, W. A.; Ibel, K. *Polymer* **1975**, *16*, 120.
(8) Kirste, R. G. In "Small-Angle X-Ray Scattering"; Brumberger, H., Ed.; Gordon and Breach: New York, 1967.
(9) Yoon, D. Y.; Flory, P. J. *Polymer* **1975**, *16*, 645.
(10) Yoon, D. Y.; Flory, P. J. *Macromolecules* **1976**, *9*, 299.
(11) Sundararajan, P. R.; Flory, P. J. *J. Am. Chem. Soc.* **1974**, *96*, 5025.
(12) Flory, P. J. "Statistical Mechanics of Chain Molecules"; Wiley-Interscience: New York, 1969.
(13) Hayashi, H.; Flory, P. J. *Macromolecules* **1983**, *16*, 1328.
(14) Yamaguchi, S.; Hayashi, H.; Hamada, F.; Nakajima, A. *Biopolymers* **1984**, *23*, 995.
(15) Flory, P. J. *Proc. Natl. Acad. Sci. U.S.A.* **1973**, *70*, 1819.
(16) Cantow, H. J.; Schulz, G. V. *Z. Phys. Chem. (Frankfurt/Main)* **1954**, *2*, 117.
(17) Furguson, R. C. *Macromolecules* **1969**, *2*, 237.
(18) Sakurada, I.; Nakajima, A.; Yoshizaki, O.; Nakamae, K. *Kolloid Z. Z Polym.* **1962**, *186*, 41.
(19) Schulz, G. V.; Wunderlich, W.; Kirste, R. G. *Makromol. Chem.* **1964**, *75*, 22.
(20) Glatter, O. *J. Appl. Crystallogr.* **1974**, *7*, 147.
(21) Kratky, O.; Pilz, I.; Schmitz, P. J. *J. Colloid Interface Sci.* **1966**, *21*, 24.
(22) Fujiwara, Y.; Flory, P. J. *Macromolecules* **1970**, *3*, 288.
(23) Brandrup, J.; Immergut, E. H., Eds. "Polymer Handbook"; Wiley-Interscience: New York, 1975.
(24) Nagai, K. *J. Chem. Phys.* **1963**, *38*, 924.
(25) Jernigan, R. L.; Flory, P. J. *J. Chem. Phys.* **1969**, *50*, 4185.
(26) Fujii, M.; Yamakawa, H. *J. Chem. Phys.* **1977**, *66*, 2578.
(27) Bondi, A. "Physical Properties of Molecular Crystals, Liquids, and Glasses"; Wiley-Interscience: New York, 1968.
(28) Flory, P. J. *Macromolecules* **1974**, *7*, 381.
(29) Yoon, D. Y.; Flory, P. J. *Macromolecules* **1976**, *9*, 294.
(30) This matrix is analogical to that in the two-state scheme.
(31) Flory, P. J.; Sundararajan, P. R.; Debolt, L. C. *J. Am. Chem. Soc.* **1974**, *96*, 5015.
(32) Flory, P. J.; Abe, Y. *J. Chem. Phys.* **1971**, *54*, 1351.
(33) Flory, P. J.; Fujiwara, Y. *Macromolecules* **1969**, *2*, 315.
(34) Gibson, K. D.; Scheraga, H. A. *Proc. Natl. Acad. Sci. U.S.A.* **1967**, *58*, 420.
(35) Hopfinger, A. J. "Conformational Properties of Macromolecules"; Academic Press: New York, 1973.
(36) Lifson, S. *J. Chem. Phys.* **1959**, *30*, 964.
(37) Schulz, G. V.; Kirste, R. G. *Z. Phys. Chem. (Frankfurt/Main)* **1961**, *30*, 171.
(38) Lovell, R.; Mitchell, R. G.; Windle, A. H. *Faraday Discuss. Chem. Soc.* **1980**, *68*, 46.
(39) Lovell, R.; Windle, A. H. *Polymer* **1981**, *22*, 175.
(40) Liquori, A. M.; Anzuino, G.; Coiro, V. M.; D'Alagni, M.; de Santis, P.; Savino, M. *Nature (London)* **1965**, *206*, 358.
(41) Bosscher, F.; Brike, G. T.; Challa, G. *Macromolecules* **1982**, *15*, 1442.
(42) Borchard, W.; Pylik, M.; Rehage, G. *Makromol. Chem.* **1971**, *145*, 169.
(43) Suzuki, H.; Hiyoshi, T.; Inagaki, H. *J. Polym. Sci., Polym. Symp.* **1977**, *No. 61*, 291.
(44) Spěváček, J.; Schneider, M.; Bohdenecký, M.; Sikora, A. *J. Polym. Sci., Polym. Phys. Ed.* **1977**, *61*, 291.
(45) Mrkivičková, L.; Stêjskal, J.; Spěváček, J.; Horska, J.; Quadrat, O. *Polymer* **1983**, *24*, 700.
(46) Fox, G.; Garret, B. S.; Goode, W. E.; Gratch, S.; Kincaid, J. F.; Spell, A.; Stroup, J. D. *J. Am. Chem. Soc.* **1958**, *80*, 1768.
(47) Kusuyama, H.; Takase, M.; Higashihata, Y.; Tseng, H. T.; Chatani, Y.; Tadokoro, H. *Polymer* **1982**, *23*, 1256.
(48) Kusuyama, H.; Miyamoto, N.; Chatani, Y.; Tadokoro, H. *Polym. Commun.* **1983**, *24*, 119.
(49) Winter, W. T.; Sarko, A. *Biopolymers* **1974**, *13*, 1461.
(50) Winter, W. T.; Sarko, A. *Biopolymers* **1974**, *13*, 1447.